High Voltage Solar Arrays for a Direct Drive Hall Effect Propulsion System*†

Gary A. Jongeward, Ira Katz**,
Ioannis G. Mikellides
Science Applications
International Corporation
10260 Campus Point Dr, MS X-1
San Diego, CA 92121
(858) 826-1624
Gary.A.Jongeward@saic.com

Melvin. R. Carruth
NASA/MSFC
(256) 544-7647
ralph.carruth@msfc.nasa.gov

David Q. King
General Dynamics
(425) 885-5000

Eugene L. Ralph
TECSTAR
(626) 286-0994
Ralphelpv@aol.com

Todd Peterson
NASA/GRC
(216) 433-5350
todd.peterson@grc.nasa.gov

IEPC-01-327

A three-year program to develop a Direct Drive Hall Effect Thruster (D2HET) system has begun as part of the NASA Advanced Cross-Enterprise Technology Development initiative. The system is expected to reduce significantly the power processing, complexity, weight, and cost over conventional low-voltage systems. The D2HET will employ solar arrays that operate at voltages greater than 300V, and will be an enabling technology for affordable planetary exploration. It will also be a stepping-stone in the production of the next generation of power systems for Earth orbiting satellites. This paper reports on initial D2HET high voltage solar array concepts, numerical models of their interactions with HET thruster plumes, and plans for plasma chamber verification tests.

INTRODUCTION

The empowerment of Hall thruster systems directly from advanced solar arrays offers considerable benefits over conventional systems. By eliminating, or significantly reducing, the power processing and distribution complexity, weight, and costs over conventional, low-voltage systems can be lowered to attractive levels for a variety of NASA's deep space missions. Such technologies may also have a wide range of applications to the commercial satellite industry.

A major concern in these systems is the potentially destructive consequences of high-voltage arcs. Nearly every satellite manufacturer has experienced design problems due to high-voltage discharges as they scale up to higher power and voltages.[1] Discharge damage to solar arrays on commercial GEO communications satellites for example, has cost more than a hundred million of dollars in losses and redesign expenses in recent years. NASA programs have also been affected. Figure 1 shows the damage on a coupon of the Terra array observed during ground tests. SAIC and NASA researchers investigated the causes of these[2] and other array failures.[3,4,5] The knowledge that was gained from these efforts was used to modify the Terra arrays before flight. The arrays are currently operating nominally on orbit. These modifications however, cost several millions of dollars.

In contrast to the system considered here the Terra solar array operates at 127V; D2HET requires 300V. The D2HET program will go beyond fixes in current systems to an entirely new design. The experience that is required to make this leap in technology draws from successful programs conducted in the past that concentrated on the elimination of array failures on satellites.[6,7] More recent efforts at GRC on direct drive power management and distribution also promise to provide critical insight.[8] Under the D2HET program,

---

* Presented as Paper IEPC-01-000 at the 27th International Electric Propulsion Conference, Pasadena, CA, 15-19 October, 2001.

** Now at JPL

the first designs will guided by our previous analyses, modeling, and testing of high voltage solar arrays in plasma environments. These efforts also led to the development of an electrostatically clean solar array coupon.[9] The interaction issues were the same as in the D2HET: arcing, parasitic currents, sputtering, thermal loads, and lifetime in the space environment from LEO out to the solar wind. Mitigation techniques for the solar array arc initiation mechanism, discovered previously during a commercial satellite anomaly investigation, will be extended to the 300V D2HET system and beyond.

This paper reviews the technology issues involved in the development of the D2HET system. Specifically, an account of our recent experience in higher voltage and power arrays is presented along with preliminary insights for +300V designs. An outline of the design methodology to be employed in this program is provided. These are accompanied by results from our plume-S/C interactions modeling efforts.

DEVELOPMENT METHODLOGY

The current goal is to design a Direct Drive Hall Effect Thruster system that provides an overall cost savings of at least 30% over conventional HET systems, 60% reduction of PPU mass, and 90% cutback of the PPU heat rejection (and associated radiator area) requirements. The major technological advance will be a 300V (or higher) solar array that will operate efficiently in both HET generated and ambient space plasmas. Design considerations include, interconnect shielding from the plasma, array string layout patterns, spacing and grouting, isolation diodes, substrate structural makeup, and grounding. A comparison of a D2HET and conventional HET system is shown in Figure 2.

Successful operation of arrays in vacuum at >300V does not necessarily guarantee operation in the space ambient and HET-generated conditions. In order to assess the effects on the arrays under different environments and mission scenarios, two satellite configurations and two HET designs are investigated using 2-D and 3-D simulation tools. The satellites are the Russian EXPRESS, a geosynchronus communications spacecraft, and the U.S. Deep Space-1. The SPT-100 and BPT-4000 thrusters have been chosen as the two representative HETs. The approach is to determine the HET environments that interact with the arrays and use the information to design and test arrays under these conditions.

Express and Deep Space-1

The two satellite models were generated using the 3-D, spacecraft interactions code EWB (Environment Work Bench). In the EXPRESS model the solar array panels were arranged according to the designs in the Express-A reports, and were configured to conduct sun-tracking rotation for mission studies. Figure 3 shows the geometry of the arrays. Figure 4 (top) shows the EWB model. Ion-flux sensors onboard the Express-A3 (Figure 5) were also incorporated in the model spacecraft. Two of these sensors, DRT1 & DRT2, were located at one edge of each solar array, 4.75 m and 9.675 m from the center. Both detectors on the EWB model were positioned on the same side for simplicity. A third detector object was also located at the DRT3-1 location The detector objects allowed for the calculation of flux to the object for comparison/validation with on-orbit measurements. Simulations have been performed during operation of the North-South station-keeping thrusters (pointing along the arrays), and the East-West station-keeping thrusters (pointing perpendicular to the array axes). In the DS-1 model the thruster was located at the bottom of the satellite. The thruster axis of symmetry was perpendicular to the solar array axis. The arrays were fixed in the orientation shown in Figure 4 (bottom) to correspond to the specific DS-1 mission.

SPT-100 and BPT-4000 Hall Effect Thrusters

In the past, numerous efforts to simulate plumes from electrostatic thrusters have allowed for the development of a complete modeling package for accessing plume interactions with spacecraft subsystems.[10,11,12,13] The experience gained over the past several years in HET plume measurements and modeling has provided a theoretical understanding of many of the interaction mechanisms. These models play an essential role in the design process because they provide the means for quantitatively estimating the HET-induced environments in which the solar arrays will operate. They also provide plasma conditions in the laboratory as the basis for testing the solar arrays and other high voltage components.
In order to assess a wider range of plume interactions with the S/C, particularly with the solar arrays, two Hall Effect Thrusters were used in the plume

simulations: the Stationary Plasma Thruster (SPT100) and the Busek-Primex Thruster (BPT4000). Operating conditions and other characteristics of these thrusters are shown in Figure 6.

ENVIRONMENT DEFINITION

Thruster Plume and Interactions with Model Spacecraft

In order to determine the HET-induced environment near the arrays a combination of simulation tools was used: a 1-D model of the HET discharge chamber, a 2-D plume code, and the 3-D interactions code.

The plume model is discussed in detail in reference 11. Briefly, the model consists of a Lagrangian primary beam algorithm and a Particle-in-Cell (PIC) solver for computing ion production from charge-exchange events. The primary beam is assumed to be a collisionless, singly-ionized, quasi-neutral plasma, expanding in a density-gradient electric field. The neutral gas density has two components in space: un-ionized beam particles and un-ionized neutralizer gas (from the hollow cathode). The beam of neutrals from the thruster is computed using an annular anode gas flow model with isotropic emission from the ring. The hollow cathode neutrals are assumed to have an isotropic emission at a constant temperature. For simulation of laboratory plumes, a third contribution to the neutrals is added based on the chamber background density, and is assumed to be uniform. Charge-exchange (CEX) is computed using a two-dimensional, R,Z-geometry PIC code. The main beam ion densities computed by the Lagrangian calculations, and the neutral gas profile, are used as input during the calculation. The code solves Poisson's equation on a finite element grid and iterates until steady state CEX densities and density-gradient potentials are self-consistent. The required conditions at the exit of the thruster are provided by a 1-D model of the acceleration channel in an SPT100 that produced good qualitative agreement with measured thruster performance in the past.[12]

Two different simulation cases of plume maps were initially performed for the SPT100 onboard the Express A2 satellite, distinguished by two mass flow rate values: 4.9 and 5.3 mg/s for the thruster and 0.49 mg/s and 0.371mg/s for the cathode-neutralizer. The higher mass flow rate case is presented here. The computed plume maps (and trajectories) are illustrated in Figure 7.

The standard 2-D plume model described above was also used in the past to explain the observed trends in the BPT4000 Hall-Effect thruster.[11] Figure 8 shows computed, plume maps one meter away from the BPT-4000 under both lab and space conditions. The CEX density in the lab was found to be more than one order of magnitude greater than it is in space due to the dominance of the background neutral gas in the chamber. The measured (integrated) ion current for a background pressure of 3e-5 torr was approximately 4.2 Amps (for collector potential of +20V). By comparison, the computed CEX ion current overestimated the measured value by about 20% (5.3Amps) due to the fact that the model does not account for the depletion of main beam ions. The calculation assumed 300V ions and employed a cross-section value of 55 $Å^2$.

The 2-D maps of the thruster exhaust were "fed" into EWB. EWB's simulation capabilities include a variety of models for assessing interactions effects from electric propulsion plumes. The thruster ion flux at any point, i, on a surface j, due to plume component k, is calculated as follows:

$$F_{ik} = \rho_{ik}\left|\vec{u}ik\right|\cos(\theta_{ik}), \quad \cos(\theta_{ik}) = \frac{\vec{n}j \cdot \vec{u}ik}{\left|\vec{n}j\right|\left|\vec{u}ik\right|} \qquad (1)$$

In equation (14), ρ_{ik} is the ion particle density and $\vec{u}_{ik}$ is the ion velocity. The angle between the surface normal vector $\vec{n}_j$, and the particle velocity is denoted by θ_{ik}. Fluxes to points on surfaces account for the interference ("blocking") by other spacecraft surfaces. Specifically, if a straight line between the point in question and the thruster orifice intercepts any other surface the flux is zero.

The sputtering of a spacecraft surface j at point i, due to energetic ion impact from the thruster is calculated based upon the material sputtering rate, R_{ij}^{S}:

$$R_{ij}^{S} = \sum_{k} Y_{ijk} F_{ik}, \quad Y_{ijk} = Y_{ijk}(E_{ik}, \theta_{ik}) \tag{2}$$

where, Y_{ijk} is the sputter yield of the material on surface j.

Depending upon the duration of thruster operation, t, the total surface erosion by direct plume impact, as well as re-deposition of sputtered particles onto other surfaces, is determined by computing a net erosion/deposition rate. The net rate is calculated as follows: for each spacecraft structure j the sputtering rates at all points are averaged to produce a source term R_j^{S}, at the centroid of that surface. This source term is then used to calculate a deposition rate at each of the grid points for all surfaces:

$$R_i^{D} = (1/2\pi) \sum_{j} R_j^{S} \Omega_{ij} \cos(\Theta) \tag{3}$$

where, Ω_{ij} is the solid angle subtended by surface j at point i, and Θ is the angle between the normal of the depositing surface and a ray from the sputtered surface centroid to point i. The net rate, R_i is then computed at each point by,

$$R_i = R_i^{D} - R_i^{S} \tag{4}$$

If $R_i > 0$ it is a deposition rate, if $R_i < 0$, it is an erosion rate. This rate is then integrated over the mission duration to get a total number of deposited particles per square meter. The integrated value is determined by calculating an average rate and then multiplied by the mission duration. This accounts for time-dependent changes in spacecraft geometry (such as solar array rotation).

The model for determining the induced torque Γ on the spacecraft during thruster operation accounts for contributions from the thrust and from exhaust impingement on surfaces:

$$\Gamma = \sum_{T} \Delta r_T \times (-f_T) + \sum_{j} \Delta r_j \times f_j \tag{5}$$

where, $\Delta r = r - r_0$ is the position vector of surface j or thruster T form a reference point with position vector, r_0. The force f_j is the momentum imparted to a surface from plume particles, per unit time. A choice to use either *specular* elastic reflection from the surface (colliding particle is reflected with the same speed and incidence angle equals the reflection angle), or diffuse reflection (based on material-dependent accommodation coefficients), is available.

Comparisons with Measurements

The results from the simulations are compared with measurements taken onboard the Express-A #2 and Express-A #3 satellites, during operation of the SPT100s. Measurements from two ion-flux sensors (DRT) onboard the Russian Express-A #2, were provided by the NASA Glenn Research Center. Data from one ion-flux sensor has been used, located at a distance of 1.352m from the thruster RT4, at an angle of approximately 80deg relative to the Xc axis. The second sensor is positioned under the MLI (multi-layer insulation) and did not provide any useful information. The sensor positions and thruster unit #4 (TU4) on the Express-A spacecraft are circled in Figure 5. Signals during this RT4's operation have been used for comparisons.

As shown in Figure 9 and Figure 10 the simulations compare well with the observed fluxes measured at a variety of angles with respect to the thruster axis. Further simulations also suggest good agreement with measured energy spectra for both the main beam and charge-exchange components.[13,14] The comparisons provide sufficient confidence in the models' predictions of the plasma environment near the arrays, and pertinent interactions with surfaces. Indeed, in addition to the high voltage-plasma interactions, a concern is posed by sputtering erosion due to the impact of highly-energetic Xe ions on spacecraft surfaces. For example, the computed expansion of the HET exhaust shown in Figure 11 for the Express configuration suggests substantial impact of the plume on the solar arrays. The obvious aversion of such potential problems by pointing the thruster away from the arrays, as in the DS-1 configuration, may not possible under certain missions. These issues will be further addressed in the D2HET program.

Calculations similar to those shown above were also performed, for both Express and DS-1, using the BPT4000 plume map. Table 1 shows a summary matrix of the interactions. The most severe interactions occur in the Express satellite while conducting north-south station keeping with the BPT 4000 thruster. This is because the BPT4000 produces the highest densities, and fires along the arrays, allowing for a large portion of highly energetic ions from the main beam to impact the arrays. The configuration of the DS-1 satellite with a SPT100 thruster has the least interaction due to the position of the thruster relative to the arrays (firing perpendicular to the array axis and in the array plane).

Table 1. Environment matrix for different HET-spacecraft combinations.

	SPT100	BPT4000
EXPRESS	Significant plasma density ($0.2e15m^{-3}$, 3m away, 0deg plume angle – $0.4e13$ m^{-3} , 3m away, 90deg plume angle) and sputtering of arrays during N-S station keeping Moderate sputtering of body	Highest densities ($0.6e15m^{-3}$, 3m away, 0deg plume angle – $0.1e14$ m^{-3} , 3m away, 90deg plume angle) during N-S station keeping Configuration with most sputtering Moderate sputtering of body
DS-1	Insignificant sputtering of arrays Moderate plasma density at arrays	Insignificant sputtering of arrays Increased plasma density over SPT100

The environment matrix in Table 1 will be used as a baseline target for the laboratory environments. The test facility, to be discussed in the next section will employ a hollow cathode plasma source to simulate the HET plumes. The higher densities ($>10^{13}$ m^{-3}) will not be attainable in the laboratory, and for these densities 2-D modeling will be used to scale the plasma interactions. Figure 13 shows an example of a 2-D calculation of the potentials in the vicinity of a solar cell edge with a front side shield covering most of the exposed edge. Comparisons of laboratory measurements with 2-D models will be performed, for current collection and surface potentials at the lower densities, and then *turn up* the density and/or temperature to HET environments.

D2HET Test Facility

A vacuum chamber at MSFC is being configured for plasma testing of design concepts. This facility is shown in Figure 14.. It is approximately 1 meter in diameter and 1.5 meters long. Two liquid nitrogen trapped diffusion pumps will provide the vacuum. A hollow cathode with an annular keeper electrode will be used to simulate HET plasma conditions in the vacuum chamber. The tips are commercially available and the source is constructed in our laboratories. Electric Propulsion Laboratory (EPL) plasma sources are also available. Typically, the source is operated with Argon. Densities in the range of 10^5 to 10^6 per cubic centimeter and electron temperatures in the order of 1 eV are produced in the vacuum chamber. With the plasma source off, a vacuum in the mid 10^{-7} torr can be achieved. With the source on, the background pressure is in the high 10^{-5} to low 10^{-4} torr.

Various diagnostics will be used to determine the plasma conditions around the array segments. Current collection by the solar array segment as a function of voltage (relative to the local plasma) will be measured and possible arcing will be detected. The surface voltage and sheath structure around solar cells will also be measured. The techniques to obtain these measurements are as follows:

- Langmuir probe to measure the plasma density, electron temperature and local plasma potential in the vicinity of the solar array segment
- Current/Voltage instrumentation oscilloscopes in conjunction with picoammeters or current amplifiers to measure the small currents collected by biased solar array segments and the applied voltage
- Oscilloscope to trigger on current surges to the solar array to detect arcing on the segment
- Video camera to view the solar array segment in the chamber during testing so that arcs on the segment can be captured by the video
- Emissive probe will be swept in front of solar array segments during test to map the sheath structure extending into the plasma as a function of voltage on the segment, the array geometry and the plasma conditions

- TREK probe-commercially available probe biases to zero electric field in order to provide non-contact surface voltage measurements.

PRELIMINARY DESIGNS

A preliminary set of candidate array designs has been selected for testing. During the initial tests mockups may be used for some designs.

Several of the solar cell arrays will be based on the Space Station array design shown in Figure 15. At the outset the existing spacing and geometry of the ISS arrays will be used due to the unique way in which they have reacted in the space environment thus far. The current collection of the ISS arrays at 160 V has been much lower than was expected based on laboratory testing and analysis. Following these initial tests other variations will also be examined. These are:

ISS specs with 8cmX8cmX8mil cells
This test article will either be a mock-up of the ISS solar array design or will be a segment supplied by Glenn Research Center. Preferably, a 4x5 cell array will be utilized to minimize the cell edge length around the edge relative to the length of cell adjacent to cell.

ISS Specification with Solid or Mesh Cover of Cell Gap
This will be the same configuration as in 2.2.1 except that the gap between cells will be covered by a grid. The electron collection is due to the fields from within the gap due to the high voltage solar cells. A grid that covers this gap will restrict the field and limit current collection from the local plasma.

ISS Specification with RTV Grouting—2X2 and 4X4 Cell Segments
This set will match specs of the ISS but with an RTV grouting applied to all gaps between the cells. This will reduce parasitic current collections and increase arc thresholds.

Large Multi-cell Cover Glass
An electrostatically clean solar array has been developed for scientific requirements. It utilizes a single large cover glass that covers a large number of solar cells at a time. This has the potential to significantly reduce high voltage cell exposure to the plasma and reduce interactions. This will be mocked up based on Composite Optics design shown in Figure 16.

Large Cover Glass Overhang and Overlap
ISS cell size will be utilized. A mocked up segment will allow examination of the effect of having a larger overhang of the cover glass. The ISS design is 3 mils. By increasing this to 10 or 20 mils and overlapping the cell edges by increasing alternating cells in height by 10 mils, the cell edges will overlap and prevent the electric field penetration into the plasma.

Thin Film Arrays
Glenn Research Center is developing several flexible thin film array technologies. An example is shown in Figure 17. Because of their advantages, we will test high voltage configurations of these arrays once samples exist. Preliminary investigations will employ mockups utilizing configurations of thin conductors covered with insulators.

Concentrators
TECSTAR's concentrator shown below in
Figure 18 allows larger string separation without loss of efficiency. This design option could be exploited to reduce inter-string and intra-string arcing.

SUMMARY

This paper reported on the initial efforts of a NASA/GRC program to develop a Direct Drive Hall Effect Thruster system design. The goal is to advance power system technology to operate free of anomalies above 300V in a HET environment.

The approach take is to; 1) Build on previous experience in D2HET demonstration programs at GRC; 2) Extend the knowledge gained during recent array anomaly analysis and mitigation efforts; 3) Define HET-satellite system configurations to baseline designs; 4) Use validated modeling tools to predict the plasma environments in which the high voltage components must operate freely of arcing and with minimal parasitic currents; 5) Stand-up a plasma test facility to test high voltage array concepts; 6) Use modeling to scale laboratory tests to high plasma density and temperate environments not attainable in the laboratory.

The initial testing of mock-up and real array coupons is ongoing as of September 2001. We plan to report on initial interaction tests in upcoming conferences.

ACKNOWLEDGMENTS

The authors wish to acknowledge the support of Thomas Kerslake and David Snyder of GRC. This works was supported under GRC contract NAS3-01100.

REFERENCES

[1] Katz, I., V. A. Davis, D. B. Snyder, "Mitigation techniques for spacecraft charging Induced arcing on solar arrays," AIAA Paper 99-0215, 36th Aerospace Sciences Meeting & Exhibit, January 1999, Reno, NV.

[2] S. Davis, R. Stillwell, W. Andiario, D. Snyder, I. Katz, "EOS-AM Solar Array Arc Mitigation Design," 99IECEC-100, to be published in the proceedings of the 1999 IECEC meeting.

[3] Katz., V.A. Davis and D.B. Snyder, Mechanism for spacecraft charging initiated destruction of solar arrays in GEO, AIAA Paper 98-1002, 35th Aerospace Sciences Meeting & Exhibit, January 12-15, 1998, Reno, NV.

[4] Katz, I., Jongeward, G. A., Davis, V. A., Parks, D. E., and Snyder, D. B., Space plasma induced arcing on high voltage solar arrays, IEEE Trans. on Electrical Insulation, 25 (2), p. 367, 1990.

[5] G. A. Jongeward, I. Katz, M. J. Mandell, D. E. Parks, The role of unneutralized surface ions in negative potential arcing, IEEE Trans. Nucl. Sci., 32, p 4087, 1985

[6] I. Katz, V.A. Davis, and D.B. Snyder, "Mechanism for Spacecraft Charging Initiated Destruction of Solar Arrays in GEO," AIAA Paper 98-1002, January 1998.

[7] C.F. Hoeber, E.A. Robertson, I. Katz, V.A. Davis, and D.B. Snyder, "Solar Array Augmented Electrostatic Discharge in GEO," ," AIAA Paper 98-1401, January 1998

[8] J. A. Hamely, J.M. Sankovic, J.R. Miller, P. Lynn, M.J. O'Neill,S.R. Oleson, "Hall Thruster Direct Drive Demonstration", AIAA Paper 97-2787, July 1997

[9] Composite Optics, Inc Final Report for NASA contract, "Development of Electrostatically Clean Solar Array Panels, NAS5-99236, May 16,2000.

[10] Davis, V.A., *et al*., "Ion Engine Generated Charge Exchange Environment: Comparison Between NSTAR Flight Data and Numerical Simulations," AIAA Paper 00-3529, July 2000.

[11] Katz, I., *et al*., "A Hall Effect Thruster Plume Model Including Large-Angle Elastic Scattering," AIAA Paper 01-3355, July 2000.

[12] Mikellides, I.G., *et al*., "A 1-D Model of the Hall-Effect Thruster with an Exhaust Region," AIAA Paper 2001-3505, July 2001.

[13] Mikellides, I.G., *et al.,* "A Hall-Effect Thruster Plume and Spacecraft Interactions Modeling Package," IEPC Paper 2001-251, Oct. 2001.

[14] David Manzella, *et al*., "Hall Thruster Plume Measurements On-board the Russian Express Satellites" IEPC Paper, 2001-44, Oct. 2001.

Figure 1. Permanent arc damage to a Terra array coupon during preflight tests.

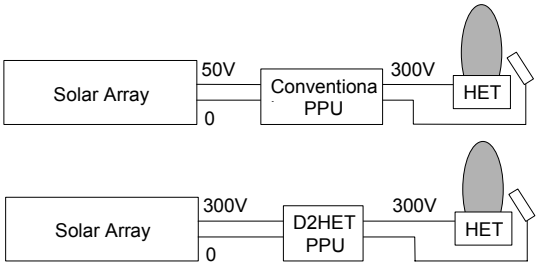

Figure 2. D2HET's high voltage solar arrays result in a smaller, lighter, simpler, PPU.

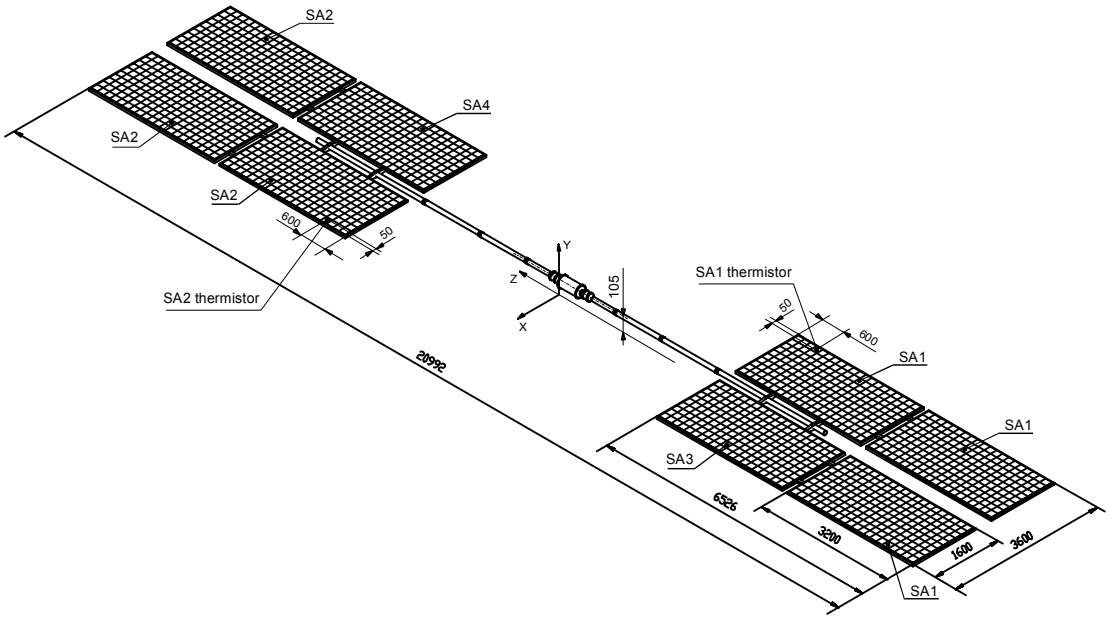

Figure 3. The Express-A solar array (showing location of temperature sensors).

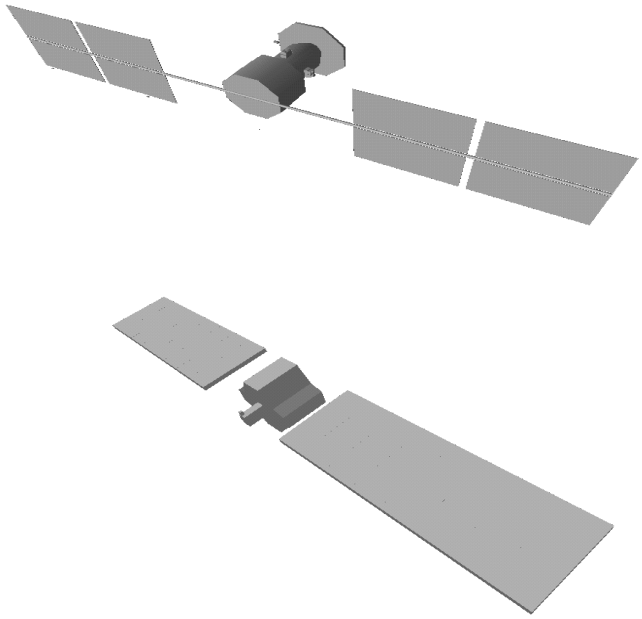

Figure 4. EWB models of EXPRESS (top) and DS-1 (bottom) used to assess HET-Array interactions.

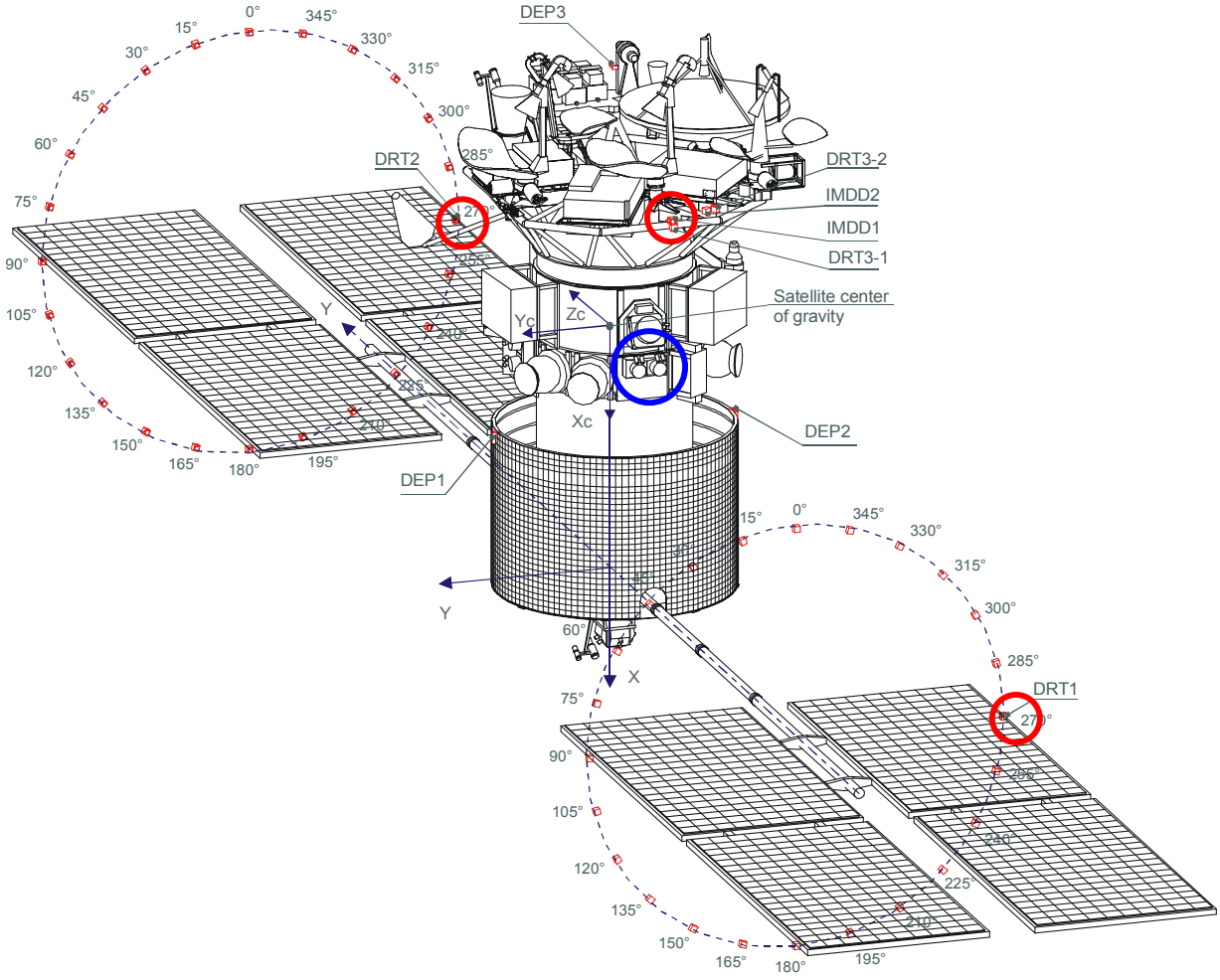

Figure 5. Location of ion-flux sensors (DRT) and SPT100 unit on the Express-A3 Satellite.

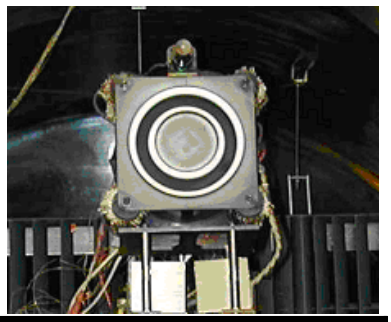

BPT4000	
Input power	4.0kW
Prop. flow rate	10.7mg/s
HC flow rate	1.2 mg/s
Discharge current	8 A
Prop. utilization	0.9
Thrust	208.3mN
Thrust eff.	0.53
Isp	1985sec

SPT100	
Input power	1.5kW
Prop. flow rate	5.2mg/s
HC flow rate	0.37 mg/s
Discharge current	4.5A
Prop. utilization	0.85-0.92
Thrust	83mN
Thrust eff.	0.48
Isp	1600sec

Figure 6. Thrusters used in the modeling and assessment of plume interactions.

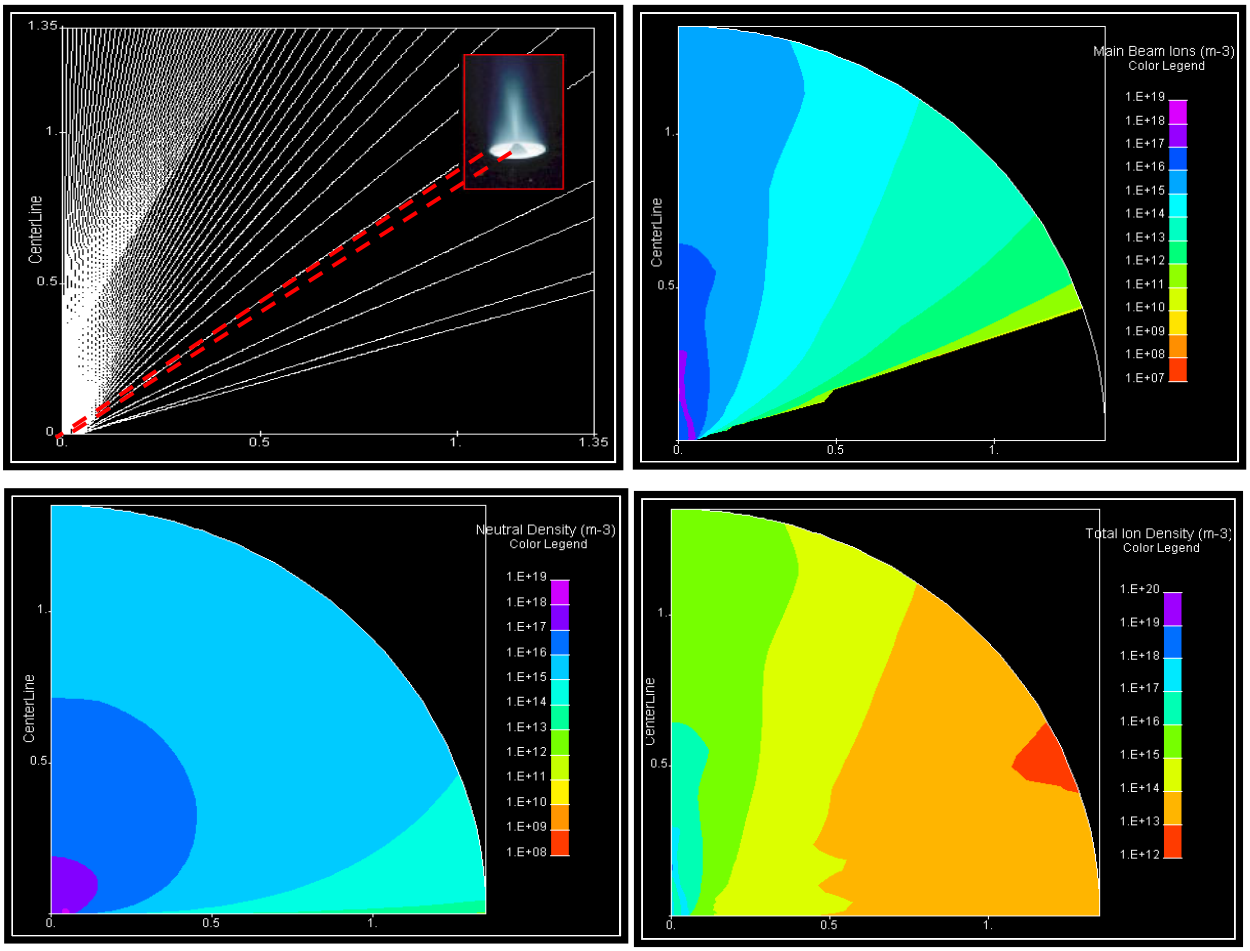

Figure 7. Results of 2-D plume simulation of SPT100 showing ion trajectories (top left), main-beam ion density (top right), neutral density (bottom left) and total ion density (bottom right).

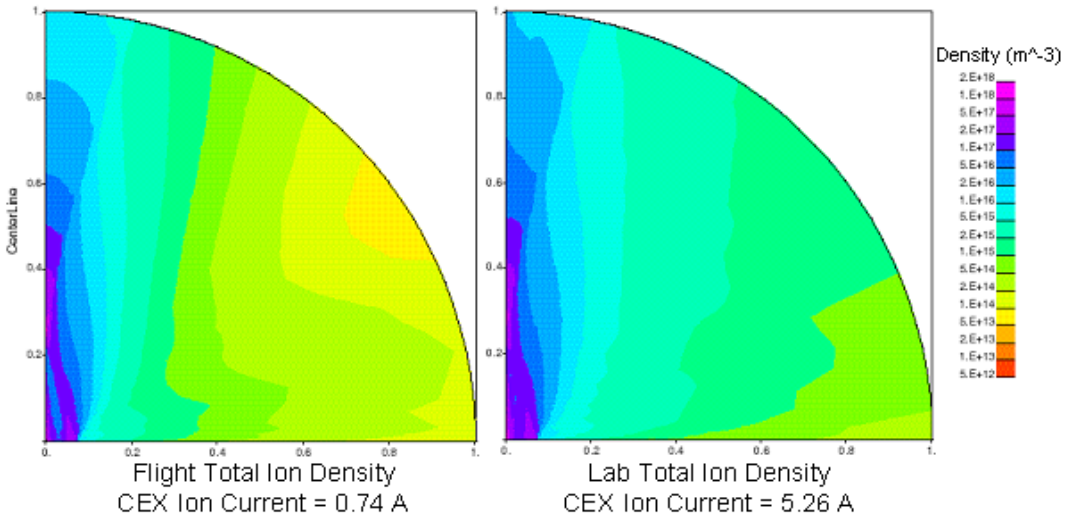

Figure 8. HET plume maps for lab and space conditions showing dominance of background density in the charge-exchange plume production.

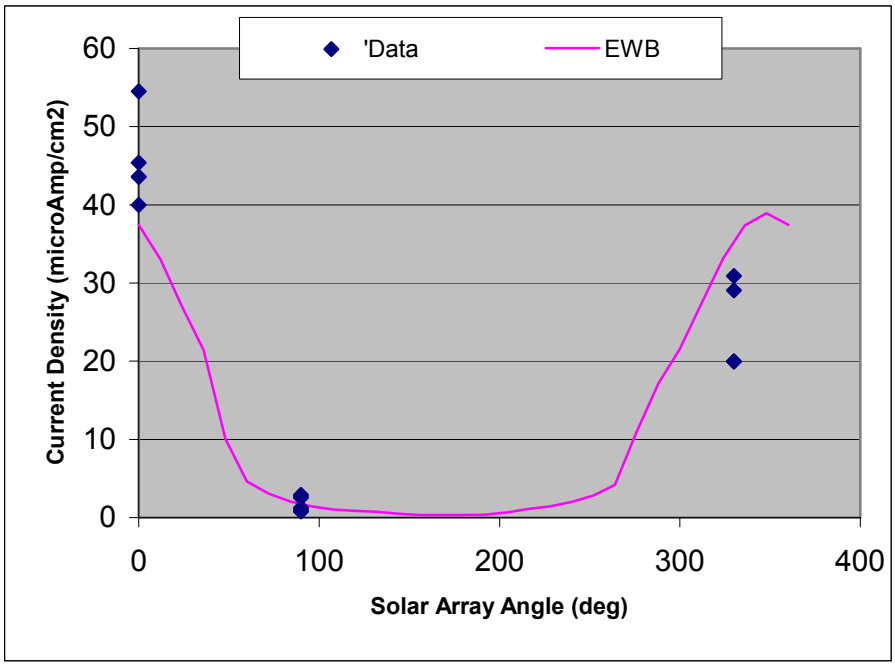

Figure 9. Comparisons of EWB calculation (solid line), incorporating the results from the 2-D plume code, with ion-flux measurements from the DRT1 sensor onboard Express A#3 during rotation of the solar arrays.

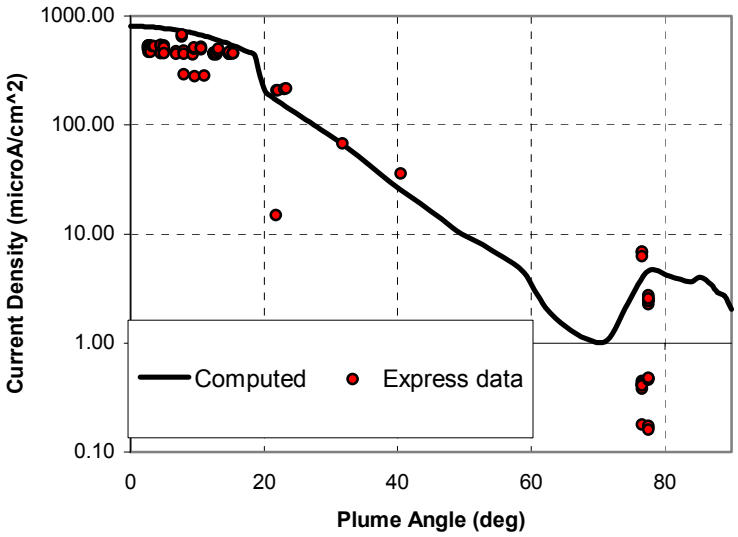

Figure 10. Comparisons between 2-D plume simulations and Express-A ion-flux data (scaled down to 1-m).

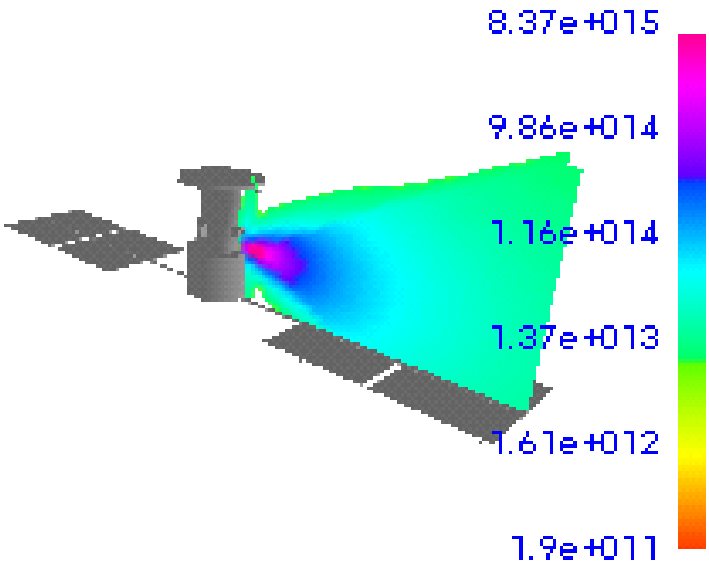

Figure 11. EWB calculation of the density in the vicinity of the EXPRESS arrays during operation of RT4 SPT-100 thruster (density is given in m^{-3}).

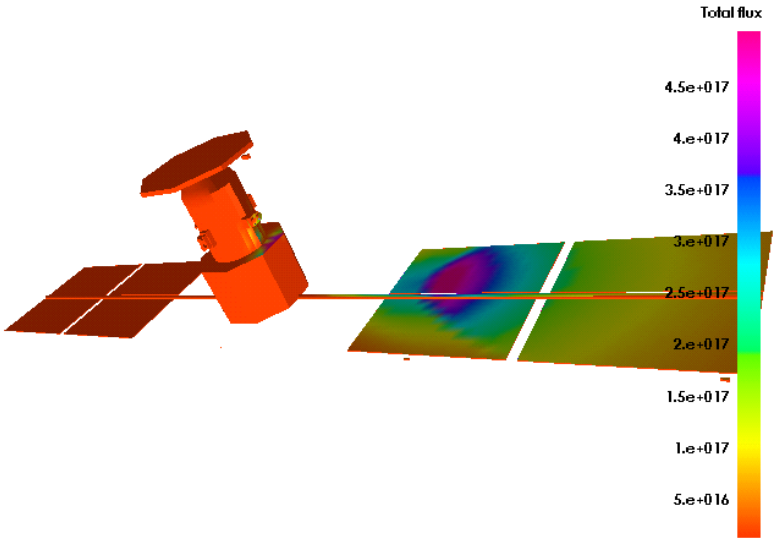

Figure 12. EWB calculation of the flux of ions to the EXPRESS array during operation of the RT4 SPT-100 thruster (flux is given in 1/s-m^2).

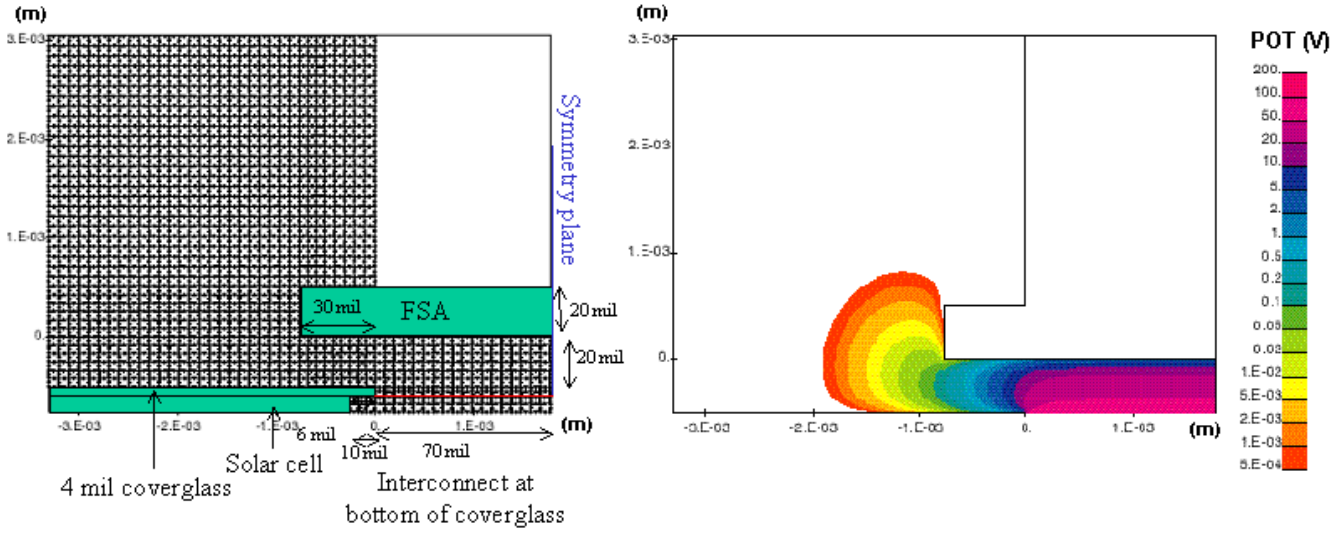

Figure 13. 2-D, solar array modeling will be used to scale plasma interactions, such as current collection, to the higher densities not attainable in the chamber. (Left: Front Side Aperture and solar array geometry and computational region. Right: computed potential profile).

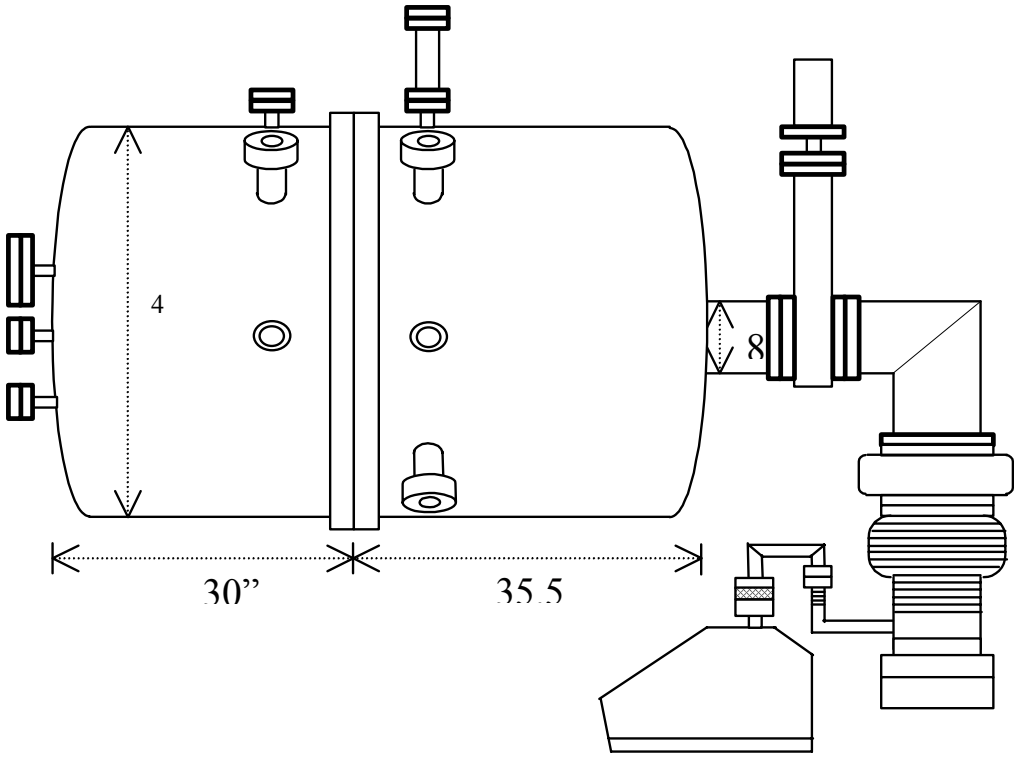

Figure 14. MSFC vacuum chamber to be used for plasma testing of candidate array designs.

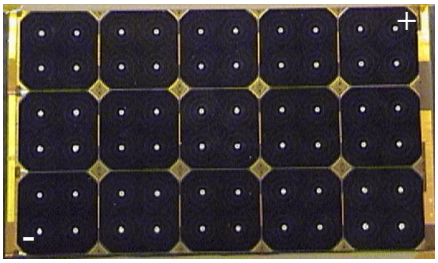

Figure 15. International Space Station array coupon showing 15 8cm x 8cm cells.

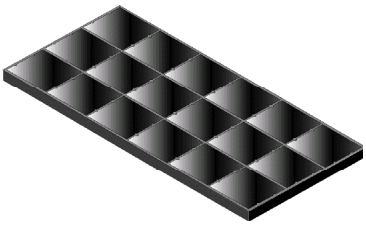

Figure 16. Front Side Array shields the exposed voltages from the plasma.

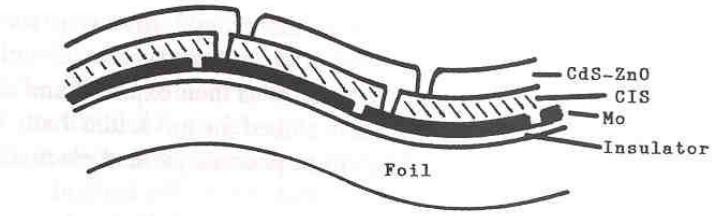

Structure of a flexible CIS submodule.

Figure 17. Flexible thin film arrays developed by GRC.

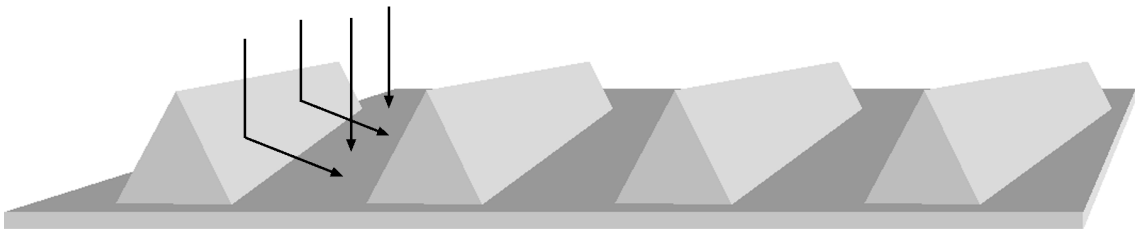

Figure 18. G-STAR concentrator of TECSTAR